

26. M. Bollig, *Risk Management in a Hazardous Environment* (Springer, New York, 2006).
27. P. Wiessner, *Curr. Anthropol.* **43**, 233 (2002).
28. C. Boehm, *Hierarchy in the Forest* (Harvard Univ. Press, Cambridge, MA, 2000).
29. M. Parker Pearson, *The Archaeology of Death and Burial* (Sutton, Stroud, UK, 1999).
30. K. Hill, A. M. Hurtado, *Ache Life History: The Ecology and Demography of a Foraging People* (Aldine de Gruyter, Berlin, 1996).
31. F. W. Marlowe, *The Hadza* (Univ. of California Press, Berkeley, CA, in press).
32. P. Wiessner, in *Politics and History in Band Societies*, E. Leacock, R. Lee, Eds. (Cambridge Univ. Press, Cambridge, 1982), pp. 61–84.
33. M. Alvard, D. Nolin, *Curr. Anthropol.* **43**, 533 (2002).
34. E. A. Smith, R. B. Bird, D. W. Bird, *Behav. Ecol.* **14**, 116 (2003).
35. R. Quinlan, *Am. Anthropol.* **108**, 464 (2006).
36. R. Sear, F. Steele, I. A. McGregor, R. Mace, *Demography* **39**, 43 (2002).
37. M. Borgerhoff Mulder, *Hum. Nat.* **20**, 130 (2009).
38. M. Gurven, H. Kaplan, A. Zelada Supa, *Am. J. Hum. Biol.* **19**, 376 (2007).
39. M. Borgerhoff Mulder, *Hum. Ecol.* **20**, 383 (1992).
40. I. Fazio, *Parental Investment Among Arab and Dazagada Herding Societies of West Chad* (VDM Verlag Dr Müller, Berlin, 2008).
41. R. McElreath, *Am. Anthropol.* **106**, 308 (2004).
42. W. Irons, *The Yomut Turkmen: A Study of Social Organization Among a Central Asian Turkic-Speaking Population* (Univ. of Michigan Museum of Anthropology, Ann Arbor, MI, 1975).
43. D. L. Leonetti, D. C. Nath, N. S. Heman, D. B. Neill, in *Grandmotherhood: The Evolutionary Significance of the Second Half of the Female Life*, E. Voland, A. Chasiotis, W. Schiefelhoevel, Eds. (Rutgers Univ. Press, New Brunswick, NJ, 2005), pp. 194–214.
44. M. K. Shenk, *Hum. Nat.* **16**, 81 (2005).
45. G. Clark, *A Farewell to Alms: A Brief Economic History of the World* (Princeton Univ. Press, Princeton, NJ, 2007).
46. M. Borgerhoff Mulder, *Curr. Anthropol.* **36**, 573 (1995).
47. E. Voland, *Behav. Ecol. Sociobiol.* **26**, 65 (1990).
48. B. S. Low, A. L. Clarke, *J. Fam. Hist.* **16**, 117 (1990).
49. The authors declare no competing interests. Financial support for this research was provided by the Behavioral Sciences Program of the Santa Fe Institute, the Russell Sage Foundation, and the NSF. We would like to thank the participating members of the populations we studied for their cooperation and M. Alexander, W. Cote, P. Lindert, C. Resnicke, T. Taylor, D. Ulibarri, and H. Wright for their contributions to this research.

## Supporting Online Material

www.sciencemag.org/cgi/content/full/326/5953/682/DC1  
Materials and Methods  
SOM Text  
Figs. S1 and S2  
Tables S1 to S13  
References

29 June 2009; accepted 29 September 2009  
10.1126/science.1178336

# The Crystal Structure of the Ribosome Bound to EF-Tu and Aminoacyl-tRNA

T. Martin Schmeing,\* Rebecca M. Voorhees,\* Ann C. Kelley, Yong-Gui Gao, Frank V. Murphy IV,† John R. Weir,‡ V. Ramakrishnan§

The ribosome selects a correct transfer RNA (tRNA) for each amino acid added to the polypeptide chain, as directed by messenger RNA. Aminoacyl-tRNA is delivered to the ribosome by elongation factor Tu (EF-Tu), which hydrolyzes guanosine triphosphate (GTP) and releases tRNA in response to codon recognition. The signaling pathway that leads to GTP hydrolysis upon codon recognition is critical to accurate decoding. Here we present the crystal structure of the ribosome complexed with EF-Tu and aminoacyl-tRNA, refined to 3.6 angstrom resolution. The structure reveals details of the tRNA distortion that allows aminoacyl-tRNA to interact simultaneously with the decoding center of the 30S subunit and EF-Tu at the factor binding site. A series of conformational changes in EF-Tu and aminoacyl-tRNA suggests a communication pathway between the decoding center and the guanosine triphosphatase center of EF-Tu.

The ribosome is the macromolecular enzyme that synthesizes proteins using aminoacyl-tRNA substrates, as directed by an mRNA template. To faithfully translate the genetic information contained in mRNA, the ribosome must select cognate tRNA by its ability to base pair with the mRNA codon, a process termed “decoding.” Elongation factor Tu (EF-Tu), a translation factor with ribosome-dependent guanosine triphosphatase (GTPase) activity, delivers aminoacyl-tRNAs to the ribosome in a ternary complex (TC) of aminoacyl-tRNA•GTP•EF-Tu (where GTP is guanosine triphosphate) and plays an active role in ensuring the fidelity of decoding. Understanding the interplay between the TC and the ribosome that leads to the accurate translation of the

mRNA message has been an active area of research for more than three decades.

Biochemical experiments have provided a wealth of information about the multistep process of tRNA discrimination by the ribosome. Initial binding of TC occurs independently of mRNA (1), after which codon-anticodon pairs are sampled at the decoding center of the 30S subunit. Correct codon-anticodon matching induces conformational changes in three 16S nucleotides—A1492, A1493, and G530 (*Escherichia coli* numbering, see table S1)—that monitor the geometry of the minor groove in the codon-anticodon helix (2) and accelerate the forward rate of selection (3). Binding of a near-cognate tRNA does not induce these changes (4), explaining why initial tRNA selection is more accurate than can be accounted for by the energetic differences between matched and mismatched anticodons alone (5). In addition to simple codon-anticodon base pairing, physical properties of the tRNA body are also important for faithful decoding (6–11). Finally, the binding energy of a cognate tRNA is used to make an important domain closure of the 30S subunit (4), moving the “shoulder” domain closer to the TC (12).

The signal that codon recognition has occurred must then be transmitted to the GTPase center of EF-Tu. The ribosome could stimulate GTP hydrolysis using two strategies: (i) by positioning catalytic residues in EF-Tu for GTP hydrolysis and (ii) by providing ribosomal components that function directly in catalysis. Domain 1 of EF-Tu is responsible for nucleotide binding, and rearrangements in this domain result in the opening of the hydrophobic gate, composed of residues Val<sup>20</sup> in the P loop and Ile<sup>60</sup> in switch I, which before activation prevents access of the catalytic His<sup>84</sup> to GTP (13). Mutation of His<sup>84</sup> results in a 10<sup>5</sup> decrease in the rate of GTP hydrolysis by EF-Tu, and this residue is thought to position and activate a water molecule to hydrolyze GTP (14). Ribosomal components implicated in GTPase activity include the sarcin-ricin loop (SRL) of 23S ribosomal RNA (rRNA), located adjacent to the nucleotide binding pocket of EF-Tu (15), ribosomal protein L7/L12, which stimulates hydrolysis 2500-fold (16), and the L11 protein and proximal rRNA (17).

Hydrolysis of GTP and release of inorganic phosphate (P<sub>i</sub>) by EF-Tu leads to lowered affinity for aminoacyl-tRNA and release from the ribosome. tRNA is then either accommodated into the peptidyl transferase center or rejected via a “proofreading” mechanism (18, 19). Proofreading and initial selection are separated by irreversible GTP hydrolysis, and their multiplicative effect accounts for the high accuracy of decoding (3, 20). Despite the wealth of biochemical data, the transmission of codon recognition to the GTPase center and the activation of GTP hydrolysis is not well understood.

Crystal structures of EF-Tu and TC have been determined for complexes with guanosine diphosphate (GDP) and GTP analogs, as well as a variety of antibiotics [(Protein Data Bank identification code 1OB2) (13, 21, 22) and references therein]. Isolated structures of EF-Tu revealed the global conformational change of domain 1 that occurs upon transition between the active (GTP) and inactive (GDP) states of the protein (13). The

MRC Laboratory of Molecular Biology, Cambridge, CB2 0QH, UK.

\*These authors contributed equally to this work.

†Present address: Northeastern Collaborative Access Team, Building 436, Argonne National Laboratory, Argonne, IL 60439, USA.

‡Present address: Max-Planck-Institut für Biochemie, Abteilung Zelluläre Strukturbiologie, Am Klopferspitz 18, Martinsried D-82152, Germany.

§To whom correspondence should be addressed. E-mail: ramakr@mrc-lmb.cam.ac.uk

conformations of switch I and switch II, which form part of the GTPase center, also depend on the nucleotide state of EF-Tu. Switch I became disordered in the complex of EF-Tu•GDP and the antibiotic methyl-kiromycin (21). TC structures reveal the substantial interaction surface between the tRNA and EF-Tu, including conserved interactions with A76 and the activated amino acid at the interface of domains 2 and 3 (22).

The complex of the TC stalled on the ribosome by the antibiotic kirromycin afforded the first visualization of EF-Tu delivering an aminoacyl-tRNA, by single particle cryo-electron microscopy (cryo-EM) (23). The tRNA was distorted into what was termed the “A/T” state (24) to interact simultaneously with the decoding center of the 30S subunit and EF-Tu, bound at the factor binding site in the intersubunit space (25). Subsequent studies produced steady improvements, and the most recent reconstructions are to beyond 7 Å resolution (26, 27). These studies provided valuable information, but precise description of subtle conformational changes, the nature of the tRNA distortion, and atomic interactions, along with the mechanistic insights to

which they lead, all require higher-resolution structures.

#### EF-Tu•tRNA Bound to the Ribosome

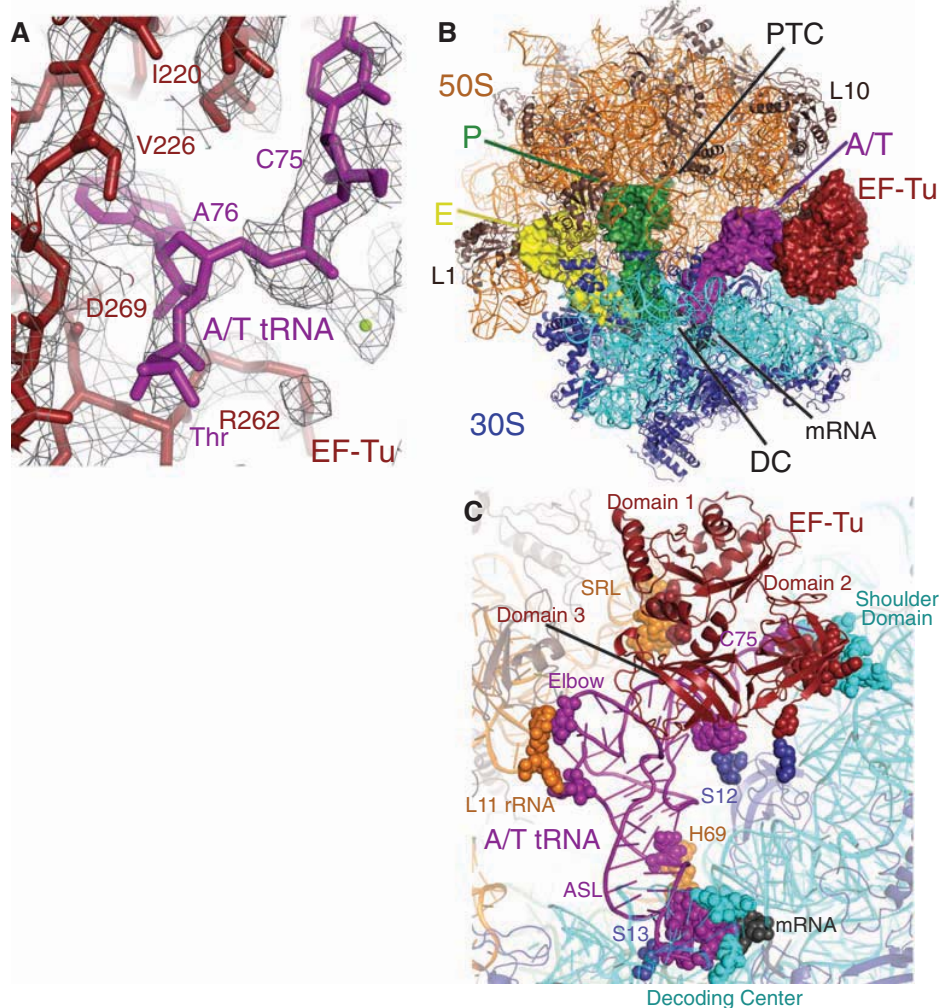
Here we present the crystal structure of the 70S ribosome from *Thermus thermophilus* in complex with tRNA<sup>Phe</sup> in the exit (E) and peptidyl (P) sites, mRNA, and the TC of EF-Tu•Thr-tRNA<sup>Thr</sup>•GDP, stabilized by the antibiotics kirromycin and paromomycin, refined to 3.6 Å resolution [ $I/\sigma(I) = 2$  at 3.75 Å] (Fig. 1 and table S1) (28). Kirromycin prevents rearrangements of EF-Tu after GTP hydrolysis and P<sub>i</sub> release, thus trapping the complex on the ribosome (29). The domain conformation of EF-Tu in this state is thought to be similar to that at the GTP transition state (30). EF-Tu and Thr-tRNA<sup>Thr</sup> have been built into electron density, with many side chains of EF-Tu, bases of tRNA, both antibiotics, and GDP clearly resolved (Fig. 1A). As expected, the ribosome is in a nonratcheted state with P- and E-site tRNAs in the classic states and a similar overall conformation to the structure containing an accommodated aminoacyl-tRNA (31) (Fig. 1B). The largest conformational changes

of the ribosome are in the L1 rRNA region and helices 43 and 44 of the 23S rRNA, which includes the L11 binding site, that become more ordered to interact with the elbow of the tRNA (Fig. 1C). The aminoacyl-tRNA is bound in the A/T state, and conformational changes in the 30S subunit indicative of cognate tRNA binding are observed including the flipping out of bases G530, A1492, and A1493 of the 16S rRNA and the “closing” of the 30S subunit (2). EF-Tu interacts with the factor binding site and the 30S “shoulder.” This overall conformation is in good agreement with previous lower-resolution cryo-EM studies (24, 26, 27).

#### Distortion of tRNA

To adopt the A/T conformation, the aminoacyl-tRNA must be distorted substantially to allow the ~30° bend required to simultaneously bind the mRNA codon and EF-Tu. There are two distinct areas of distortion in the tRNA body: (i) a bend in a 13-nucleotide region of the anticodon stem and (ii) a change in the positioning of the D stem with respect to the acceptor- and T-stem contiguous stack. The very 3' end of the

**Fig. 1.** Structure of EF-Tu and aminoacyl-tRNA bound to the ribosome. **(A)** Representative electron density from an unbiased difference Fourier map displayed at 1.3 $\sigma$ , with the refined model of EF-Tu (red) and Thr-tRNA<sup>Thr</sup> (purple). **(B)** Overall view of the complex, with EF-Tu and tRNAs depicted as surfaces, and rRNA and protein as cartoons. PTC, peptidyl transferase center; DC, decoding center. **(C)** Contacts between TC and the ribosome, with interacting residues shown as spheres.



tRNA is also distorted, as the backbone of residues 72 to 75 has shifted by up to 6 Å, and nucleotides C72 and C75 have swung outward. Although this conformation has an important mechanistic role (described below), it is not directly connected to the bent conformation of the tRNA body. The acceptor helix and anticodon adopt the canonical conformation, and the anticodon stem loop (ASL) of the A/T tRNA interacts with the decoding center in the same way as fully accommodated cognate aminoacyl-tRNA (A/A tRNA) (31) (Fig. 2A).

The anticodon stem distortion involves a reduction of helical twist and a widening of the phosphate backbone. The distortion begins at base pair 30:40, where the tRNA adopts a smooth bend involving nucleotides 25 to 30 and 40 to 48, rather than a kink as previously proposed (24). The helix in this region becomes under-twisted by up to 14°, from base pairs 30:40 through 25:45, to facilitate this bend (Fig. 2B). The distortion also includes a widening of the

strands directly above the anticodon stem, as the phosphate-phosphate distance of nucleotides 25•45 and 26•44 are ~2 and 1 Å wider than in canonical tRNA. The observed widening explains the biochemical result that mutation of the 27:43 base pair gives an error-prone phenotype (9); weakening of this base pair could decrease the energy required to separate the strands at the adjacent nucleotides, allowing the distortion to occur more easily and, thus, the binding of mismatched tRNA. Indeed, the 27:43 base pair appears to be disrupted in the structure of the A/T tRNA, though the electron density for the base of C27 is not well-defined.

Ribosome binding also causes a second region of distortion, which moves the D stem away from the T- and acceptor-stem stack (Fig. 2C). This movement does not affect the canonical stack between the T and acceptor stems, which superimpose very well between the isolated and ribosomal-bound TCs (phosphorous atom root mean square deviation of 1.3 Å). The distortion

of the A/T tRNA begins at the junction of the acceptor stem and D stem, around unpaired nucleotides 8 and 9, which results in a ~5 Å swing of the D arm. This rearrangement separates the 15:48 and 16:59 base pairs, but the displacement is smaller at the distal bases of the D loop (~G19), and the elbow interactions are largely unaltered.

The fact that codon recognition involves a tRNA distortion with a rearrangement of the D stem explains several experimental observations (Fig. 2D). A proflavin moiety, inserted at position 16 or 17, produces a fluorescent signal upon codon recognition (1), which is easily explained by the ~5 Å displacement of these nucleotides in the distorted A/T tRNA. The Hirsh suppressor tRNA is a tRNA<sup>Trp</sup> with a G24A mutation that allows Trp incorporation at UGA stop codons (6). G24 is normally base paired to C11, but in the distorted conformation the tRNA backbone across these nucleotides is ~1 Å farther apart than in a canonical tRNA, suggesting how the Hirsh suppressor can more easily sample the distorted conformation (7, 8). A chemical cross-link between D-stem nucleotide 13 and nucleotide 8 (which is directly adjacent to the acceptor stem) occurs less frequently in the Hirsh tRNA background (32); these nucleotides separate in the distorted conformation. Conversely, the 8-to-13 cross-link would reduce the propensity for adopting the distortion required for decoding and has been shown to limit the miscoding activity of the Hirsh suppressor tRNA (10). The disruption of the 9:12:23 triple also gives a phenotype similar to the Hirsh suppressor (8). Interruption of this stabilizing interaction would facilitate deformation of the tRNA in the D-stem region. However, as the triple is intact in the A/T state, mutation of this base triple would probably allow formation of an altered distortion that achieves a similar bend to that observed for a wild-type tRNA. These mutations within the tRNA body would reduce the energetic penalty for distortion, which is normally precisely balanced against the energy derived from cognate codon-anticodon interaction. Thus, productive binding of TC and GTP hydrolysis can occur in these cases for even a near-cognate codon-anticodon interaction, as the energetic barrier for adopting the A/T conformation has been reduced.

Although the proposed nature of the tRNA distortion differed in older cryo-EM studies, its general description in the most recent cryo-EM work is similar to that observed in the present x-ray crystal structure (26, 27). Although a distortion of the anticodon stem was observed, the widening of the tRNA above the anticodon stem was not detected, and the extent of the D-stem movement is considerably larger than reported.

#### Ribosomal Stabilization of Distorted tRNA: Few But Important Interactions

The highly distorted tRNA must be stabilized by interactions with the ribosome and EF-Tu. The structure reveals that the A/T tRNA interacts primarily with the decoding center and EF-Tu

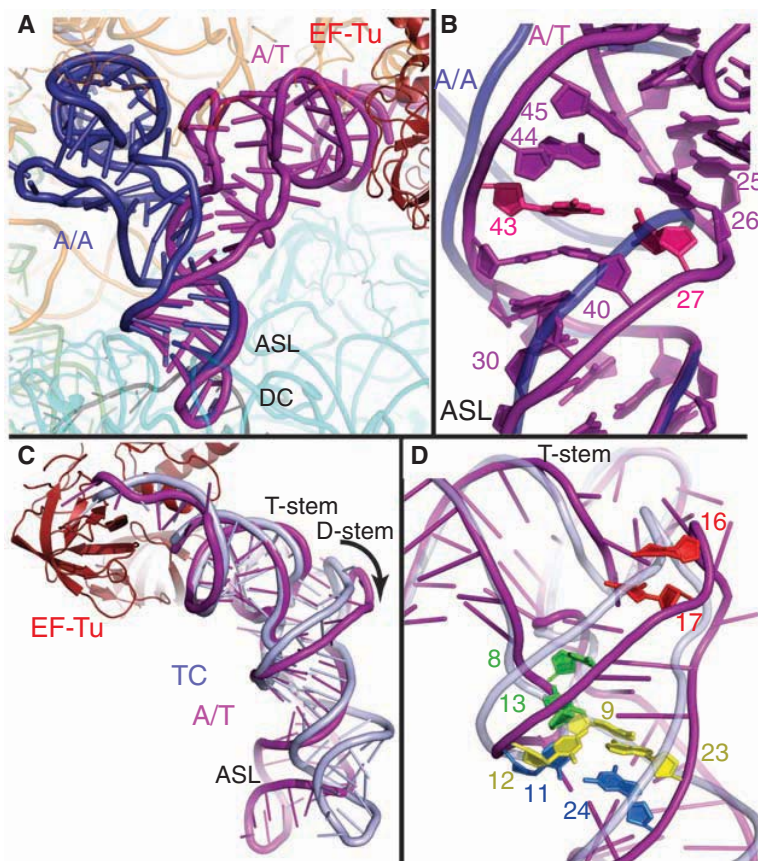


**Fig. 2.** Distortion of aminoacyl-tRNA in the A/T state. **(A)** Comparison of the A/T tRNA (purple) with the fully accommodated canonical A/A tRNA (dark blue) (31) shows the overall extent of the tRNA distortion. **(B)** The structures diverge in the ASL with a reduction of helical twist after base pair 30:40 and separation of the phosphate-sugar backbones at nucleotides 25 to 45 and 26 to 44. Disruption of the 27:43 base pair (pink) (9) would facilitate this strand separation. **(C)** Comparison of the A/T tRNA with tRNA of the isolated TC (light blue) (22) highlights the swinging out and ~5 Å shift of D-arm nucleotides. **(D)** The distortion rationalizes data pertaining to proflavin insertions at nucleotides 16 and 17 (bright red) (1), cross-linking of nucleotides 8 and 13 (green) (32), and mutations of the Hirsh base pair 24:11 (blue) (6, 8) and 9:12:23 triple (yellow) (8).

while forming very few additional contacts with the ribosome (Fig. 1C). The decoding center interacts with the tRNA in a near identical manner to accommodate tRNA (31). A single additional sugar packing interaction between residue C25 of the tRNA and C1914 of 23S rRNA helix 69 is observed in this region.

In addition to the decoding center, the tRNA interacts with three regions of the ribosome: (i) the shoulder domain of the 16S rRNA, (ii) ribosomal protein S12, and (iii) the L11 region of 23S rRNA (Fig. 1C). Distortion in the 3' end of the A/T tRNA involving residues 72 through 75 allows C75 to pack between EF-Tu residue 219 and the flipped base of A55, a residue that is 99.5% conserved in all species of known sequence (Fig. 3). Although A55 changes conformation, the rest of helix 5 of 16S rRNA is largely unaltered. S12 contacts the tRNA at the acceptor-arm/D-stem junction. In this region, the side chain of Gln<sup>74</sup> is within hydrogen-bonding distance of the 2'OH of A67, and the side chain of His<sup>76</sup> interacts with the sugar of residue U68. These two S12 residues form part of the highly conserved QEH sequence (33). Mutation of His<sup>76</sup> leads to streptomycin-resistance, suggesting that this contact is important for proper TC binding (34). The S12 interactions were previously reported to be with tRNA residue 69 (26). In addition, EF-Tu contacts S12 with a single salt bridge between Glu<sup>249</sup> of domain 2 of EF-Tu and Lys<sup>119</sup> of S12.

The L11 rRNA interacts with the tRNA elbow at residue dihydroU20 (which is within hydrogen-bonding distance of U1068) and C56 through a packing interaction with A1067. The latter interaction is consistent with biochemical data showing that mutation of A1067U resulted in a threefold decrease in the rate of TC binding to the ribosome and a twofold decrease in the rate of GTP hydrolysis for cognate tRNA (35).

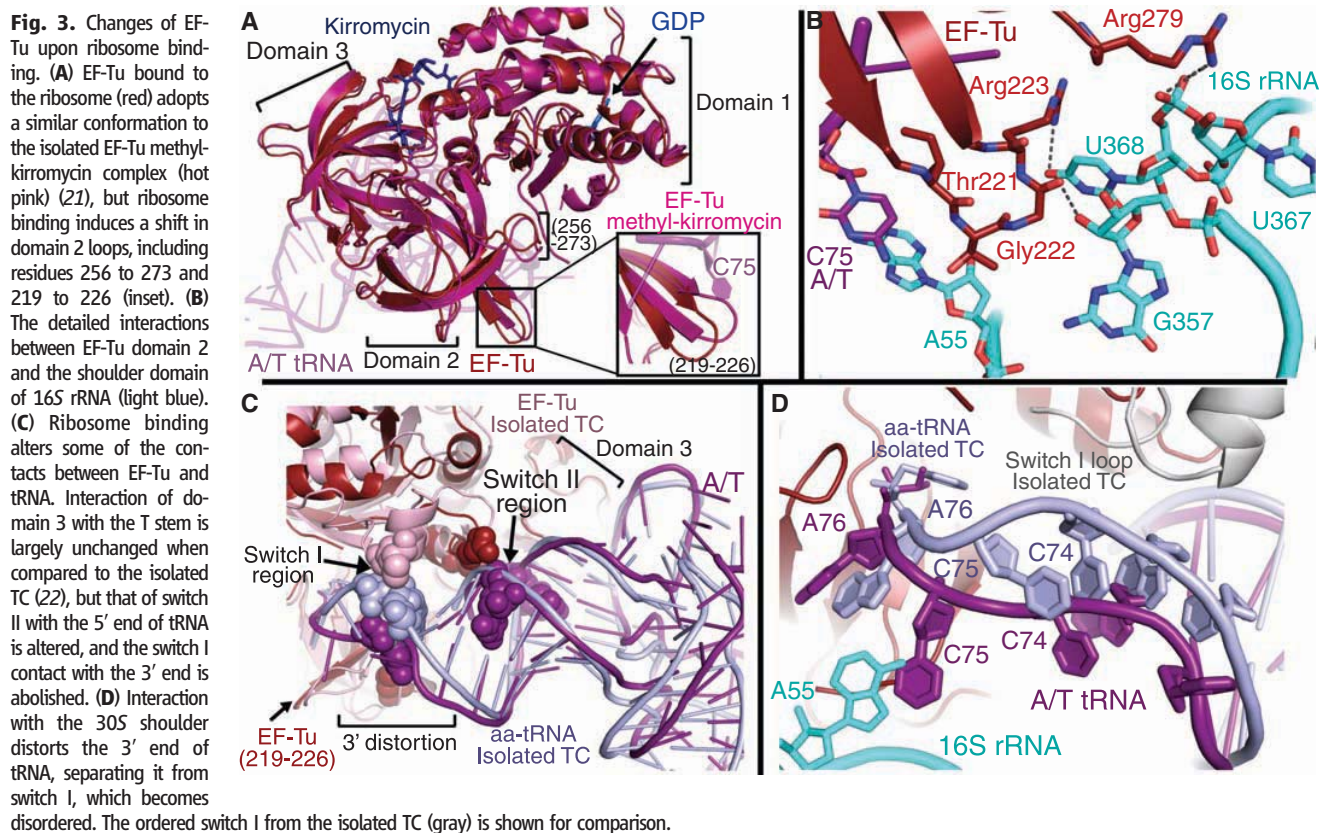
Considering only these few interactions outside the decoding center, the surface area of the A/T tRNA buried by the ribosome is only 482 Å<sup>2</sup>. The most extensive interactions of the tRNA are those with EF-Tu, which bury 1540 Å<sup>2</sup> of surface area. The movement of the strained tRNA into the peptidyl transferase center upon release of EF-Tu would require disruption of only a few interactions with the ribosome, an energetic barrier that should be easily surmountable by the potential energy stored in the strained tRNA.

### An Important Interaction Between Domain 2 and the 16S rRNA

The overall domain orientation of the ribosome-bound EF-Tu is very similar to that of the isolated methyl-kiromycin structure (21, 27); however, a small concerted conformational change is observed in surface residues of domain 2 (Fig. 3A). Whereas those residues forming the interface between domains 2 and 3 remain unaltered, domain 2 residues 256 to 273 and 219 to 226, the latter composing a  $\beta$  turn near the 3' end of the A/T

tRNA, shift to allow two loops of EF-Tu to contact the 16S rRNA shoulder (Fig. 3, A and B). These interactions are facilitated by the domain closure of the 30S subunit, which moves the 16S rRNA toward EF-Tu. As these movements are not observed in the isolated structures of EF-Tu, even when similarly bound to both GDP and kirromycin, they are presumably a result of ribosome binding. Residues 278 to 281 interact with 16S rRNA residues 367 and 368 via packing, in addition to hydrogen bonding between Arg<sup>279</sup> and U368. The second of these loops of EF-Tu packs into a pocket of 16S rRNA made by residues 55 and 56, 357 and 358, and 368. Hydrophobic interactions include those between Thr<sup>221</sup> and 16S residues A55 and U56 and between Gly<sup>222</sup> and U368, whereas hydrogen-bonding interactions occur between Arg<sup>223</sup> and Gly<sup>222</sup> and U368 and G357, respectively. This loop undergoes the most marked change upon ribosome binding, and the contacts may be of particular importance, as four of the seven residues between 219 and 226 are more than 99% conserved in all species, including humans. Furthermore, hydrogen-bonding interactions with both loops of EF-Tu occur with residue U368, which is 99.7% conserved across all species.

Mutational and biochemical data highlight the importance of the interaction between domain 2 of EF-Tu and the shoulder of the 30S subunit. Mutation of Gly<sup>222</sup> to an aspartate prevents hydrolysis of GTP by EF-Tu, and thus



protein synthesis, at physiological  $Mg^{2+}$  concentrations (36, 37). At  $Mg^{2+}$  concentrations above 10 mM, the Gly<sup>222</sup> → Asp<sup>222</sup> (G222D) mutant EF-Tu can hydrolyze GTP and allow tRNA accommodation, although via a somewhat altered pathway (36). Further, kinetic data suggested that the G222D mutant EF-Tu was specifically deficient in its ability to transmit codon-anticodon recognition to the GTPase center, perhaps by preventing a conformational change in EF-Tu (36). Replacement of the highly conserved Gly<sup>222</sup> would probably prevent the conformational change in this loop required for interaction with the 16S rRNA. Additionally, placing a large, negatively charged aspartate in a position that abuts the phosphate backbone of the 16S rRNA would be electrostatically unfavorable. However, at  $Mg^{2+}$  concentrations above 10 mM, this negative charge is probably screened by the divalent cations, partially rescuing the deficiency of the G222D mutant EF-Tu.

#### Shoulder Binding Alters Certain Interactions of EF-Tu with tRNA

Upon ribosome binding, local conformational changes of EF-Tu in both domain 2 and switch II alter the nature of a specific subset of the contacts between EF-Tu and the tRNA (Fig. 3C). Despite the suggestion from a cryo-EM study (26), the contacts between EF-Tu and the aminoacyl-

tRNA are similar to those observed in the isolated structure of TC for much of the binding surface, including those involving the tRNA T-stem and parts of the acceptor stem (22). Likewise, interactions with the activated amino acid of aminoacyl-tRNA are maintained, including a hydrogen bond between Arg<sup>262</sup> and the backbone carbonyl and Asn<sup>273</sup> with the primary amine, as well as several hydrogen bonds with A76.

In solution, EF-Tu protects the labile ester bond of aminoacyl-tRNA and must continue to prevent hydrolysis of this bond upon binding to the ribosome. Maintaining these interactions with the amino acid while also allowing the conformational change of domain 2 toward the 16S rRNA may in part require the observed distortion of the 3' end of the A/T tRNA (Fig. 3) and the previously unseen EF-Tu/tRNA interactions. This distortion of the tRNA between residues 72 and 75 moves the bases of C74 and C75 to interact with Arg<sup>283</sup> and Thr<sup>219</sup>-Ile<sup>220</sup>, respectively (fig. S1), and shifts the tRNA backbone 5 to 6 Å away from the position of switch I in the isolated GDPNP•TC (GDPNP is a GTP analog) (Fig. 3D) (22). This would disrupt the interaction of tRNA residues 73 and 74 with switch I, perhaps leading to the disordering of switch I, for which we see no electron density.

Ribosome binding shifts the switch II loop toward the backbone of the tRNA [this motion is

also mimicked by binding of kirromycin (Protein Data Bank identification code 1OB2)], allowing interaction between the phosphate oxygen of C65 with the side chain of Lys<sup>89</sup>. In a recent cryo-EM study, however, the authors suggested, based on a comparison with the isolated kirromycin-TC structure, that upon ribosome binding the acceptor arm of the tRNA shifted closer to switch II of EF-Tu, facilitating formation of an interaction between the conserved Asp<sup>86</sup> and the tRNA (26). However, a negatively charged Asp side chain would interact with the phosphate backbone in a repulsive manner. We find the acceptor arm of the tRNA not to be distorted from the canonical structure, evidenced by the superimposition of this region with that from the isolated TC (22) (Fig. 3C). With this comparison, it is instead a local movement of the switch II loop (including Asp<sup>86</sup>) that allows the altered interaction of switch II with the acceptor stem.

#### GTPase Activation by the Ribosome

Along with the P loop, switch I and switch II are functional components of the GTPase center of EF-Tu. GTP is protected from hydrolysis by a hydrophobic gate of Ile<sup>60</sup> (switch I) and Val<sup>20</sup> (P loop) (13). During ribosome-induced GTP hydrolysis, this gate is opened, allowing putative catalytic residues Gly<sup>83</sup> and His<sup>84</sup> of switch II to interact with the  $\gamma$ -phosphate or nucleophilic

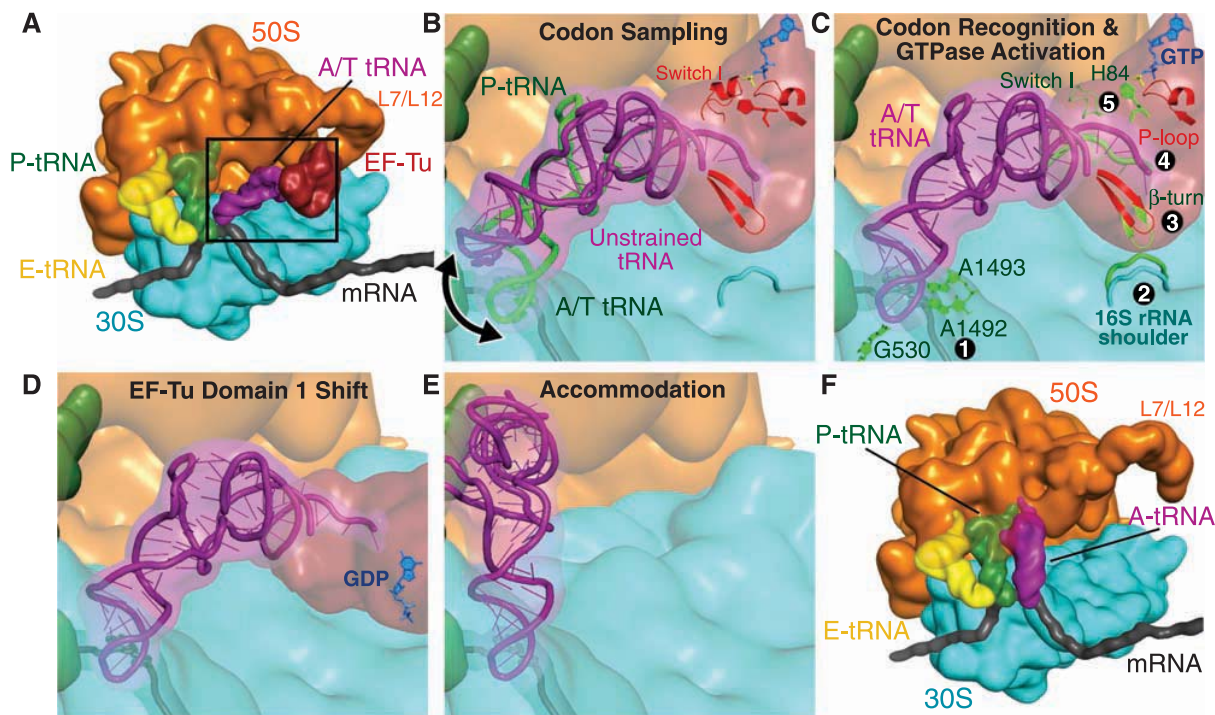


**Fig. 4.** Schematic representation of the decoding pathway. (A) The L7/L12 stalk recruits TC to a ribosome with deacylated tRNA in the E site and peptidyl-tRNA in the P site. The black frame represents the enlarged area depicted in (B) to (E). (B) The tRNA samples codon-to-anticodon pairing until a match (C) is sensed, by decoding center nucleotides 530, 1492, and 1493 (1). Codon recognition triggers domain closure of the 30S subunit (2), bringing the

shoulder domain into contact with EF-Tu and shifting the  $\beta$  loop at 230 to 237 of domain 2 (3). This changes the conformation of the acceptor end of the tRNA (4), disrupting its contacts with switch I, which becomes disordered (5), opening the hydrophobic gate to allow His<sup>84</sup> to catalyze GTP hydrolysis. (D) GTP hydrolysis and  $P_i$  release cause domain rearrangement of EF-Tu, leading to its release from the ribosome and (E and F) accommodation of aminoacyl-tRNA.

water (13, 14). In the present structure, the catalytic His<sup>84</sup> is positioned away from the G nucleotide in its inactivated position (22), consistent with the post-GTPase state of this complex (fig. S2). The switch II loop and the P loop are well ordered, but no density is observed for the switch I region from residues 42 to 65, including Ile<sup>60</sup> of the hydrophobic gate. This disordering of switch I may be the mechanism of opening the hydrophobic gate, as observed in the isolated structure of EF-Tu in complex with GDP and methyl-kinomycin (21).

The disorder of switch I seen here is in contrast to the recent cryo-EM structure of the ribosome bound to the TC in the same state (26) that reports weak density for an alternate conformation of switch I interacting with helices 8 and 14 of the 16S rRNA. There is no evidence for this conformation in the current study, even in electron density maps calculated to low resolution and displayed at low threshold, consistent with another cryo-EM structure (27).

Perhaps because the reported structure does not depict the transition state of the GTP hydrolysis reaction, we cannot identify ribosomal components that could directly function in catalysis, despite the proposal that additional catalytic groups may be involved (38). No density was observed for ribosomal protein L7/L12, which is known to be important for stimulating GTP hydrolysis by the ribosome, although perhaps through indirect action (16). Also important for GTP hydrolysis is the SRL of the 23S rRNA, which interacts with domain 1 of EF-Tu. No conformational changes of the SRL are observed when compared to that containing an ASL in the A site (39). However, the catalytic His<sup>84</sup> interacts with the 2'OH of G2661, probably holding the residue in its inactivated state (fig. S2). Additionally, EF-Tu residue His<sup>19</sup> is within hydrogen-bonding distance of a phosphate oxygen of G2661 of the SRL. Mutation of SRL residue G2661C results in hyperaccurate ribosomes, perhaps by disrupting an interaction between EF-Tu and the SRL, further destabilizing the binding of near-cognate tRNA (40). Though Val<sup>20</sup> (P loop), one part of the hydrophobic gate, is positioned close to these interactions, the SRL does not seem to be directly involved in opening the hydrophobic gate. Furthermore, the closest nucleotide of the SRL is ~5.5 Å from the GDP sugar, which would be too far to be directly involved in stimulating GTP hydrolysis.

### Insights into the Decoding Pathway

The crystal structure of EF-Tu trapped on the ribosome provides an opportunity to analyze the complete decoding pathway in its structural context and to propose the mechanism by which codon-anticodon recognition is communicated to the GTPase center more than 80 Å away (Fig. 4 and movie S1).

**Initial binding and sampling.** The multi-meric L7/L12 recruits TC for initial reversible and

mRNA-independent binding (Fig. 4A) (1, 41). In the initial TC conformation, the position of the tRNA allows sampling of codon-anticodon matches without excessive tRNA strain (Fig. 4B and fig. S3) (36).

**Codon recognition and GTPase activation.** The aminoacyl-tRNA samples a strained conformation until codon-anticodon recognition takes place (42), which results in the 30S subunit domain closure (Fig. 4C) (2). The precisely tuned flexibility of the tRNA facilitates its distortion (11). EF-Tu is pulled into its productive conformation by interactions with the distorted tRNA and by contacts with the ribosome.

Binding of EF-Tu induces a shift of regions of domain 2—including the β turn composed of residues 219 to 226—toward the now closed 16S rRNA. This leads to a ~5 Å distortion of the 3' end of the tRNA (residues 72 to 75), which disrupts interactions between the tRNA and switch I loop. Loss of these stabilizing interactions leads to disordering of switch I, which opens the hydrophobic gate, thereby transmitting the signal that codon recognition has taken place to the heart of the GTPase center. This proposal explains why cleavage of switch I between residues Arg<sup>57</sup> and Gly<sup>58</sup> or Lys<sup>51</sup> and Ala<sup>52</sup> causes defects in ribosome-induced GTP hydrolysis by EF-Tu (43), as these cleavages would prevent transmission of the signal from the 3' end of the tRNA to the GTPase center.

Opening of the hydrophobic gate allows putative catalytic residues Gly<sup>83</sup> and His<sup>84</sup> of switch II to interact with the γ-phosphate and/or activate a water molecule, triggering GTP hydrolysis (13, 14, 44).

**Nucleotide-induced conformation change of EF-Tu.** After GTP hydrolysis and P<sub>i</sub> release, EF-Tu undergoes a conformational change to its GDP form, which involves a ~100° swing of the domain 1 relative to domains 2 and 3 (Fig. 4D) (13). This movement would disrupt the interactions of domain 1 with the SRL, as well as those between switch II and the tRNA acceptor arm, separating TC and leading to dissociation of EF-Tu from the ribosome.

**Accommodation and proofreading.** In the absence of EF-Tu, the few interactions between the distorted tRNA and the ribosome leave a largely clear path to the peptidyl transferase center (PTC) (Figs. 1C and 4E). The energetics of accommodation must be finely balanced, as near-cognate tRNAs are discriminated against at this second checkpoint in decoding (3). A near-cognate tRNA would have weaker interactions with the decoding center, as it cannot induce the closed 30S conformation that is characteristic of cognate tRNA binding (4). Therefore, as the tRNA reverts to its relaxed form, near-cognate tRNA might more easily disengage from the decoding center rather than swing into the PTC, providing the molecular mechanism for proofreading (4, 45). Once accommodation is complete, peptide bond formation is very rapid, and the proper incoming amino acid is added to the

nascent peptide chain, thus achieving the goal of decoding.

### References and Notes

- M. V. Rodnina, T. Pape, R. Fricke, L. Kuhn, W. Wintermeyer, *J. Biol. Chem.* **271**, 646 (1996).
- J. M. Ogle *et al.*, *Science* **292**, 897 (2001).
- K. B. Gromadski, M. V. Rodnina, *Mol. Cell* **13**, 191 (2004).
- J. M. Ogle, F. V. Murphy, M. J. Tarry, V. Ramakrishnan, *Cell* **111**, 721 (2002).
- T. Xia *et al.*, *Biochemistry* **37**, 14719 (1998).
- D. Hirsh, *Nature* **228**, 57 (1970).
- L. Cochella, R. Green, *Science* **308**, 1178 (2005).
- D. Smith, M. Yarus, *J. Mol. Biol.* **206**, 503 (1989).
- D. W. Schultz, M. Yarus, *J. Mol. Biol.* **235**, 1381 (1994).
- J. Vacher, R. H. Buckingham, *J. Mol. Biol.* **129**, 287 (1979).
- O. Piepenburg *et al.*, *Biochemistry* **39**, 1734 (2000).
- J. M. Ogle, V. Ramakrishnan, *Annu. Rev. Biochem.* **74**, 129 (2005).
- H. Berchtold *et al.*, *Nature* **365**, 126 (1993).
- T. Daviter, H. J. Wieden, M. V. Rodnina, *J. Mol. Biol.* **332**, 689 (2003).
- D. Moazed, J. M. Robertson, H. F. Noller, *Nature* **334**, 362 (1988).
- D. Mohr, W. Wintermeyer, M. V. Rodnina, *Biochemistry* **41**, 12520 (2002).
- H. R. Bourne, P. A. Sanders, F. McCormick, *Nature* **349**, 117 (1991).
- R. C. Thompson, P. J. Stone, *Proc. Natl. Acad. Sci. U.S.A.* **74**, 198 (1977).
- T. Ruusala, M. Ehrenberg, C. G. Kurland, *EMBO J.* **1**, 741 (1982).
- S. C. Blanchard, R. L. Gonzalez, H. D. Kim, S. Chu, J. D. Puglisi, *Nat. Struct. Mol. Biol.* **11**, 1008 (2004).
- L. Vogeley, G. J. Palm, J. R. Mesters, R. Hilgenfeld, *J. Biol. Chem.* **276**, 17149 (2001).
- P. Nissen *et al.*, *Science* **270**, 1464 (1995).
- H. Stark *et al.*, *Nature* **389**, 403 (1997).
- M. Valle *et al.*, *EMBO J.* **21**, 3557 (2002).
- D. Moazed, H. F. Noller, *Cell* **57**, 585 (1989).
- E. Villa *et al.*, *Proc. Natl. Acad. Sci. U.S.A.* **106**, 1063 (2009).
- J. C. Schuette *et al.*, *EMBO J.* **28**, 755 (2009).
- Materials and methods are available as supporting material on Science Online.
- U. Kothe, M. V. Rodnina, *Biochemistry* **45**, 12767 (2006).
- M. V. Rodnina, R. Fricke, W. Wintermeyer, *Biochemistry* **33**, 12267 (1994).
- R. M. Voorhees, A. Weixlbaumer, D. Loakes, A. C. Kelley, V. Ramakrishnan, *Nat. Struct. Mol. Biol.* **16**, 528 (2009).
- A. Favre, R. Buckingham, G. Thomas, *Nucleic Acids Res.* **2**, 1421 (1975).
- Single-letter abbreviations for the amino acid residues are as follows: A, Ala; C, Cys; D, Asp; E, Glu; F, Phe; G, Gly; H, His; I, Ile; K, Lys; L, Leu; M, Met; N, Asn; P, Pro; Q, Gln; R, Arg; S, Ser; T, Thr; V, Val; W, Trp; and Y, Tyr.
- S. T. Gregory, J. F. Carr, A. E. Dahlberg, *RNA* **15**, 208 (2009).
- U. Saarma, J. Remme, M. Ehrenberg, N. Bilgin, *J. Mol. Biol.* **272**, 327 (1997).
- E. Vorstenbosch, T. Pape, M. V. Rodnina, B. Kraal, W. Wintermeyer, *EMBO J.* **15**, 6766 (1996).
- G. W. Swart, A. Parmeggiani, B. Kraal, L. Bosch, *Biochemistry* **26**, 2047 (1987).
- M. V. Rodnina, *Proc. Natl. Acad. Sci. U.S.A.* **106**, 969 (2009).
- M. Selmer *et al.*, *Science* **313**, 1935 (2006); published online 7 September 2006 (10.1126/science.1131127).
- N. Bilgin, M. Ehrenberg, *J. Mol. Biol.* **235**, 813 (1994).
- M. Diaconu *et al.*, *Cell* **121**, 991 (2005).
- T. H. Lee, S. C. Blanchard, H. D. Kim, J. D. Puglisi, S. Chu, *Proc. Natl. Acad. Sci. U.S.A.* **104**, 13661 (2007).
- W. Zeidler *et al.*, *Eur. J. Biochem.* **239**, 265 (1996).
- C. Knudsen, H. J. Wieden, M. V. Rodnina, *J. Biol. Chem.* **276**, 22183 (2001).
- T. Pape, W. Wintermeyer, M. Rodnina, *EMBO J.* **18**, 3800 (1999).
- We thank M. M. Babu and P. Lukavsky for help with data analysis, G. Leonard and S. Brockhauser for their guidance and advice with data collection at the European Synchrotron Light Source beamline ID14.4.

C. Schulze-Briese and A. Pauluhn for help with initial diffraction studies performed at the Swiss Light Source, and L. Ulisko for preparation of additional images. This work was supported by the Medical Research Council U.K., the Wellcome Trust, the Agouron Institute, and the Louis-Jeantet Foundation. R.M.V. is the recipient of a Gates-Cambridge scholarship; T.M.S. received support from the Human Frontiers Science Program Organization and Emmanuel College, University of Cambridge; and

V.R. holds stock options and is on the Scientific Advisory Board of Rib-X Pharmaceuticals, a company dedicated to making antibiotics that target the ribosome. The structure has been deposited at the Protein Data Bank with accession codes 2WRN, 2WRO, 2WRQ, and 2WRR.

**Supporting Online Material**  
www.sciencemag.org/cgi/content/full/1179700/DC1  
Materials and Methods

Figs. S1 to S3  
Tables S1 and S2  
References  
Movie S1

27 July 2009; accepted 9 September 2009  
Published online 15 October 2009;  
10.1126/science.1179700  
Include this information when citing this paper.

# The Structure of the Ribosome with Elongation Factor G Trapped in the Posttranslocational State

Yong-Gui Gao, Maria Selmer,\* Christine M. Dunham,† Albert Weixlbaumer,‡  
Ann C. Kelley, V. Ramakrishnan§

Elongation factor G (EF-G) is a guanosine triphosphatase (GTPase) that plays a crucial role in the translocation of transfer RNAs (tRNAs) and messenger RNA (mRNA) during translation by the ribosome. We report a crystal structure refined to 3.6 angstrom resolution of the ribosome trapped with EF-G in the posttranslocational state using the antibiotic fusidic acid. Fusidic acid traps EF-G in a conformation intermediate between the guanosine triphosphate and guanosine diphosphate forms. The interaction of EF-G with ribosomal elements implicated in stimulating catalysis, such as the L10-L12 stalk and the L11 region, and of domain IV of EF-G with the tRNA at the peptidyl-tRNA binding site (P site) and with mRNA shed light on the role of these elements in EF-G function. The stabilization of the mobile stalks of the ribosome also results in a more complete description of its structure.

The ribosome is the large molecular machine that uses an mRNA template to synthesize proteins, in a process referred to as translation. Ribosomes from all species consist of a large and a small subunit, which are termed 50S and 30S subunits in bacteria and consist of roughly two-thirds RNA and one-third protein. The last decade has seen a revolutionary change in our understanding of translation, largely as a result of the determination of high-resolution structures of the ribosomal subunits, as well as, more recently, the entire ribosome (1). Protein factors play crucial roles in all stages of translation, which can be divided roughly into initiation, elongation, and termination. The hydrolysis of guanosine 5'-triphosphate (GTP) by factors is required in all three stages of translation.

At the heart of translation is the elongation cycle, which consists of sequential addition of amino acids to the growing polypeptide chain directed by the mRNA codons. This process is catalyzed by two guanosine triphosphatase (GTPase) factors, elongation factors Tu (EF-Tu) and G (EF-G).

At the beginning of the cycle, a nascent peptide chain linked to a tRNA is bound in the peptidyl-tRNA binding site (P site) of the ribosome, whereas the A site remains empty. The incoming aminoacyl-tRNA is delivered to the aminoacyl-tRNA site (A site) of the ribosome as a ternary complex with EF-Tu and GTP. After GTP hydrolysis and peptidyl transfer, the nascent peptide chain is linked to the new amino acid on the A-site tRNA through the formation of a peptide bond, leaving the P-site tRNA deacylated.

This assembly of tRNAs and mRNA must then move with respect to the ribosome by one codon in a process known as translocation, which is catalyzed by EF-G. In the first step of translocation, the aminoacyl ends of the tRNAs move with respect to the 50S subunit, so that the P- and A-site tRNAs move to the E (exit) and P sites, respectively, creating hybrid P/E and A/P states of the tRNAs (2). The formation of the intermediate states of tRNA is coupled to a rotation or ratcheting of about 6° of the 30S and 50S subunits relative to each other (3, 4). The binding of EF-G to this ratcheted state catalyzes the second step of translocation, which involves movement of the mRNA and the anticodon stem-loops of the tRNAs with respect to the 30S subunit, accompanied by a resetting of the ratchet. The hydrolysis of GTP by EF-G is known to precede and accelerate this second step (5). Translocation completes the elongation cycle and leaves the ribosome with tRNAs in the E and P sites and an empty A site ready for the next amino-acyl

tRNA. In addition to its role in translocation, EF-G is also required for ribosome recycling, where it acts in conjunction with ribosome recycling factor (1).

Although biochemical studies have elucidated the overall role of EF-G in translocation, understanding the detailed mechanism of the process requires knowledge of the precise interactions EF-G makes with the ribosome in various states of translocation. Crystal structures of EF-G with and without bound guanosine diphosphate (GDP) have been determined (6, 7). The structure of the ternary complex of EF-Tu with tRNA and the GTP analog GTPNP showed a surprising similarity in shape to that of EF-G (8). The GTPase domains of the two factors are similar, and domain IV of EF-G protrudes from the body of the molecule in a manner similar to that of the tRNA anticodon stem-loop, which suggests that EF-G and the ternary complex bind the ribosome in a similar way.

To date, the main structural data on the binding of any GTPase factors to the ribosome come from cryo-electron microscopy (cryo-EM). The complex of EF-G with the ribosome has been solved in both the GTP and GDP states of the factor (9–13). These structures show that the conformation of EF-G on the ribosome is significantly altered from that of the isolated crystal structures. They also reveal the orientation of the factor on the ribosome in the pre- and post-GTP hydrolysis states and the conformational changes in the ribosome itself that accompany binding of EF-G. Further details of the mechanism of translocation require higher-resolution structures, but crystallization of the ribosome in complex with any GTPase factor has been elusive.

In this study, we report a new crystal form of the 70S ribosome made possible by use of a mutant ribosome that eliminates the steric clash that excludes GTPase factors in all previously published crystal forms (14). We have used this form to determine the structure of the posttranslocation state of the ribosome in complex with EF-G and fusidic acid, an antibiotic that allows GTP hydrolysis and translocation by EF-G but prevents its release from the ribosome. The structure, which is refined to 3.6 Å ( $I/\sigma = 2$  at 3.7 Å), reveals conformational changes in the ribosome involved in GTPase activation; details of the interaction of domain IV of EF-G with the ribosome, mRNA, and tRNA; and insights into the mechanism of fusidic acid, which functions only in complex with EF-G bound to the ribosome.

MRC Laboratory of Molecular Biology, Hills Road, Cambridge, CB2 0QH, UK.

\*Present address: Department of Cell and Molecular Biology, Uppsala University, Box 596, Uppsala, SE 751 24, Sweden.

†Present address: Department of Biochemistry, Emory University School of Medicine, Atlanta, GA 30322, USA.

‡Present address: The Rockefeller University, Box 224, New York, NY 10065, USA.

§To whom correspondence should be addressed. E-mail: ramak@mrc-lmb.cam.ac.uk



[www.sciencemag.org/cgi/content/full/1179700/DC1](http://www.sciencemag.org/cgi/content/full/1179700/DC1)

## Supporting Online Material for

### **The Crystal Structure of the Ribosome Bound to EF-Tu and Aminoacyl-tRNA**

T. Martin Schmeing, Rebecca M. Voorhees, Ann C. Kelley, Yong-Gui Gao, Frank V. Murphy IV, John R. Weir, V. Ramakrishnan\*

\*To whom correspondence should be addressed. E-mail: [ramakr@mrc-lmb.cam.ac.uk](mailto:ramakr@mrc-lmb.cam.ac.uk)

Published 15 October 2009 on *Science* Express  
DOI: 10.1126/science.1179700

**This PDF file includes:**

Materials and Methods  
Figs. S1 to S3  
Tables S1 and S2  
References

**Other Supporting Online Material for this manuscript includes the following:** (available at [www.sciencemag.org/cgi/content/full/1179700/DC1](http://www.sciencemag.org/cgi/content/full/1179700/DC1))

Movie S1

## **Supplemental information**

### **Materials and Methods**

#### Purification of ribosomes, tRNA, and mRNA

Mutant 70S *Thermus thermophilus* ribosomes containing a C-terminal truncation of the L9 protein were obtained as described (1). Cells were grown at the Bioexpression and Fermentation Facility at the University of Georgia and ribosomes were purified as previously reported (2). tRNAs were purified from *E. coli* as described (2), and mRNA was obtained from Dharmacon of sequence

5' GGCAAGGAGGUAAAAUGUUCACCAAA 3'.

#### Complex formation and crystallization

Complexes were prepared with His-tagged EF-Tu as described by Schuette et al. (3). The isolated ternary complex (EF-Tu•GTP•Thr-tRNA<sup>Thr</sup>) was assembled by incubation of EF-Tu (120  $\mu$ M) with GTP (6 mM) and a tRNA charging reaction of tRNA<sup>Thr</sup> (26  $\mu$ M), threonyl-synthetase (50 nM), threonine (0.4 mM), ATP (6mM), phosphoenolpyruvate (6 mM), pyruvate kinase (0.02 mg/ml), and pyrophosphatase (0.01 mg/ml) in a buffer of 10 mM K-HEPES pH 7.5, 15 mM MgOAc<sub>2</sub>, 50 mM KCl, 10 mM NH<sub>4</sub>Cl, and 6 mM  $\beta$ -mercaptoethanol, for 30 minutes at 37°C. Separately, an initiation complex was formed in the same buffer at 55° C containing ribosomes, mRNA, and tRNA<sup>Phe</sup> as described previously (2). The initiation complex was then cooled on ice and kirromycin and paromomycin were added at 50 and 100  $\mu$ M, respectively. Paromomycin was included because it increases the stability of the TC-ribosome complex. Initiation and ternary complexes were combined and incubated for 30 minutes at 37°C. Purification of ribosomes bound to ternary complex by “pull-down” was as described (4), except that the elution from Ni<sup>+</sup>-NTA was with 50 mM His adjusted to pH 6.5. The eluted fractions were pelleted through a 1.1 M sucrose cushion containing antibiotics and the buffer described above at pH 6.5, overnight at 86,000 g, to remove excess ternary complex.

The pelleted 70S complexes were resuspended at concentrations of 3.7-4  $\mu$ M, in a buffer containing 10 mM K-HEPES pH 6.5, 13 mM MgOAc<sub>2</sub>, 50 mM KCl, 10 mM NH<sub>4</sub>Cl, and 1 mM tris(2-carboxyethyl)phosphine), 50  $\mu$ M kirromycin, and 100  $\mu$ M paromomycin. Following addition of equimolar tRNA<sup>Phe</sup> and the detergent HEGA-9 to a concentration of 46 mM, crystals were grown via vapor diffusion in sitting drop trays by addition of 3  $\mu$ L reservoir (100 mM MES pH 6.3, 22-25 mM KCl, 50 mM sucrose, 1% glycerol, and 5.4% (w/v) PEG20K) to 3  $\mu$ L of the 70S-TC sample. Crystals with needle or plate morphology were visible within hours and grew to full size (~1000  $\mu$ m x 500  $\mu$ m x 30  $\mu$ m) within one week. Crystals were cryo-protected stepwise until reaching a final solution containing 100 mM MES pH 6.3, 33 mM KCl, 50 mM sucrose, 1.1% glycerol, 6.0% (w/v) PEG20K, 15 mM MgOAc<sub>2</sub>, and 30% (w/v) PEG400, in which they were incubated overnight. Crystals were harvested and frozen by plunging into liquid nitrogen.

## Data collection and refinement

The crystals are in space group  $P2_1$ , with unit cell dimensions  $a=289.566$   $b=268.363$   $c=403.884$ ,  $\beta=91.011$ . Small variations in the crystallization conditions led to an alternative, related crystal form, also in  $P2_1$ , where the length of the  $c$  axis has been halved. The two forms are related by a small translation of the ribosome, which breaks the crystallographic symmetry, leading to two ribosome molecules in the larger asymmetric unit.

X-ray diffraction data were collected on ID 14-4 at the European Synchrotron Light Source, Grenoble, France. Data were collected in  $10\text{-}30^\circ$  wedges on 12 separate crystals due to the extreme radiation sensitivity of the crystals. Merging wedges of diffraction data likely led to an increase in R factors. Data were integrated and scaled using XDS (5). The structure was determined by molecular replacement using the program CNS (6) and the high-resolution structure of the 70S ribosome as a starting model (2) with corrections as reported (7). Refinement was carried out using the programs CNS (6) and Phenix (8) using the following general scheme: rigid body refinement of each of the 70S ribosomes in the asymmetric unit; followed by an additional rigid body refinement in which each of the rRNA domains, ribosomal proteins, ligands, and tRNAs were defined as separate rigid groups; and finally, rounds of energy minimization and B-factor refinement. Noncrystallographic restraints were used during refinement. Iterative rounds of building and refinement were carried out resulting in a final model containing P- and E-site tRNAs, mRNA, the ternary complex, and the antibiotic ligands. Parallel refinements that did not include TC were performed to yield unbiased density maps. All displayed electron density maps were calculated using the program CNS (6). Figures were generated with Pymol (Delano Scientific). Helical parameter measurements were obtained using the program Curves, and buried surface areas were obtained using the program CNS. Sequence conservation statistics for rRNA were obtained from The Comparative RNA Web Site (<http://www.rna.cccb.utexas.edu/>), and for EF-Tu were calculated using sequences obtained from Microbial Genome Database for Comparative Analysis (<http://mbgd.genome.ad.jp/>) and the National Center for Biotechnology Information.

**Table s1.** Relationship between *Thermus thermophilus* and *E. coli* numbering of EF-Tu and ribosomal protein S12. The text refers to the *E. coli* numbering for ease of reference to the literature, but the pdb deposition is in native *T. thermophilus* numbering for EF-Tu and ribosomal proteins. rRNA has been converted to *E. coli* numbering for deposition.

<b><u>EF-Tu</u></b>	
<i>E. coli</i>	<i>T.thermophilus</i>
19	19
20	20
42	42
51	52
52	53
53	54
57	58
58	59
60	61
65	66
83	84
84	85
86	87
89	90
114	115
219	230
220	231
221	232
222	233
223	234
226	237
249	261
256	268
259	271
262	274
273	285
278	290
279	291
281	293
283	295
<b><u>S12</u></b>	
<i>E. coli</i>	<i>T.thermophilus</i>
74	78
76	80
119	123

**Table s2.** Summary of crystallographic data and refinement

<b>Data collection</b>	<b>70S-TC (merged from 12 crystals)</b>
Space Group	P2 <sub>1</sub>
Cell dimensions	
<i>a</i> , <i>b</i> , <i>c</i> (Å)	<i>a</i> =289.566 <i>b</i> =268.363 <i>c</i> =403.884
$\alpha$ , $\beta$ , $\gamma$ (°)	$\alpha$ =90.000 $\beta$ =91.011 $\gamma$ =90.000
Resolution (Å)	50-3.6 (3.9-3.6) *
R <sub>sym</sub>	21.9 (76.9)
<i>I</i> / $\sigma$ <i>I</i>	6.15 (1.73) *
Completeness (%)	93.6(85.7)
Redundancy	6.0 (5.2)
<b>Refinement</b>	
Resolution (Å)	50.0-3.6
No. unique reflections	665,418
<i>R</i> <sub>work</sub> / <i>R</i> <sub>free</sub>	28.3/30.8
No. atoms	
RNA	205,034
Protein	100,772
<i>B</i> -factors	
RNA	104
Protein	111
R.m.s deviations	
Bond lengths (Å)	0.008
Bond angles (°)	1.2

\* *I*/ $\sigma$ *I* =2 at 3.75 Å resolution.

## Supplemental Figures

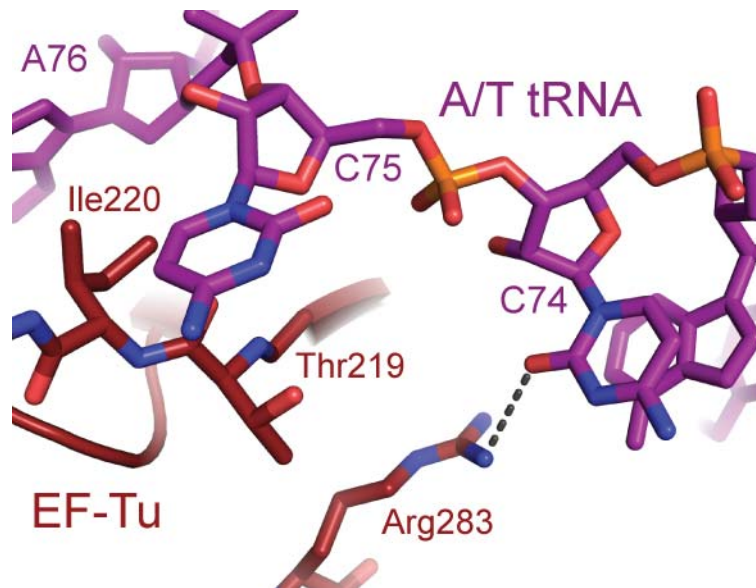


**fig s1.** Interactions of the 3' end of the A/T tRNA with EF-Tu. Upon binding of the TC to the ribosome, the 3' end of the aminoacyl-tRNA becomes distorted between residues 72-75. This distortion allows tRNA residues C74 and C75 to form stabilizing interactions with EF-Tu. More specifically, residue C75 packs against residues Ile220 and Thr219 of EF-Tu while C74 moves within hydrogen-bonding distance of Arg283.

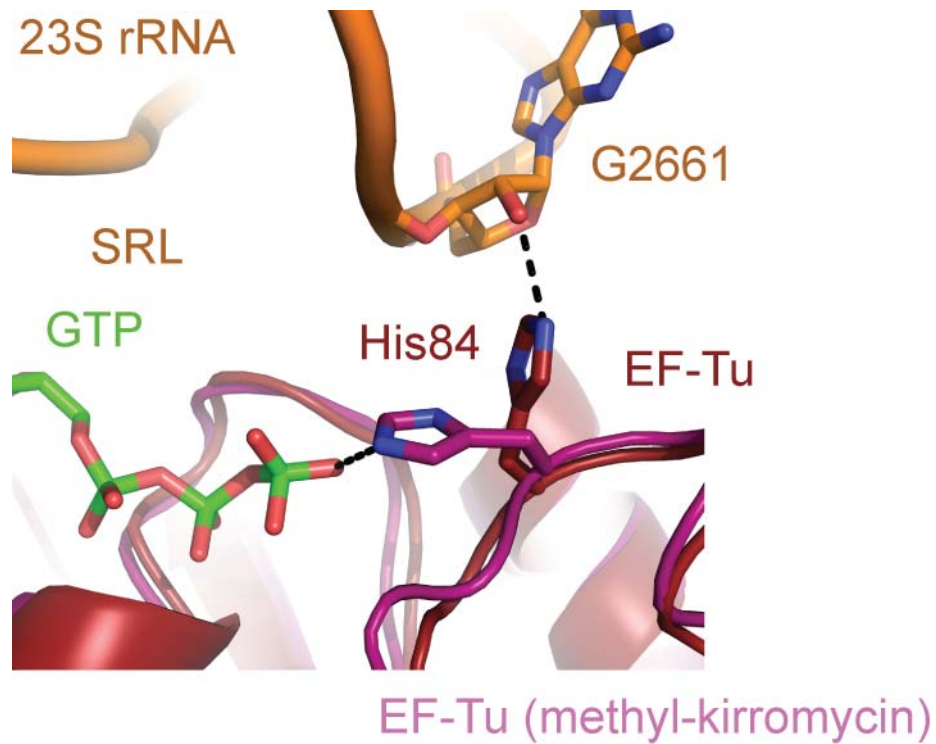


**fig s2.** Interaction of the EF-Tu catalytic residue His84 with SRL nucleotide G2661. His84 is within hydrogen bonding distance of the 2' OH of G2661 of the sarcin ricin loop. In the structure of EF-Tu in complex with aurodox, His84 is positioned towards the (modeled)  $\gamma$ -phosphate of GTP, and may aid in GTP hydrolysis (9) (10).

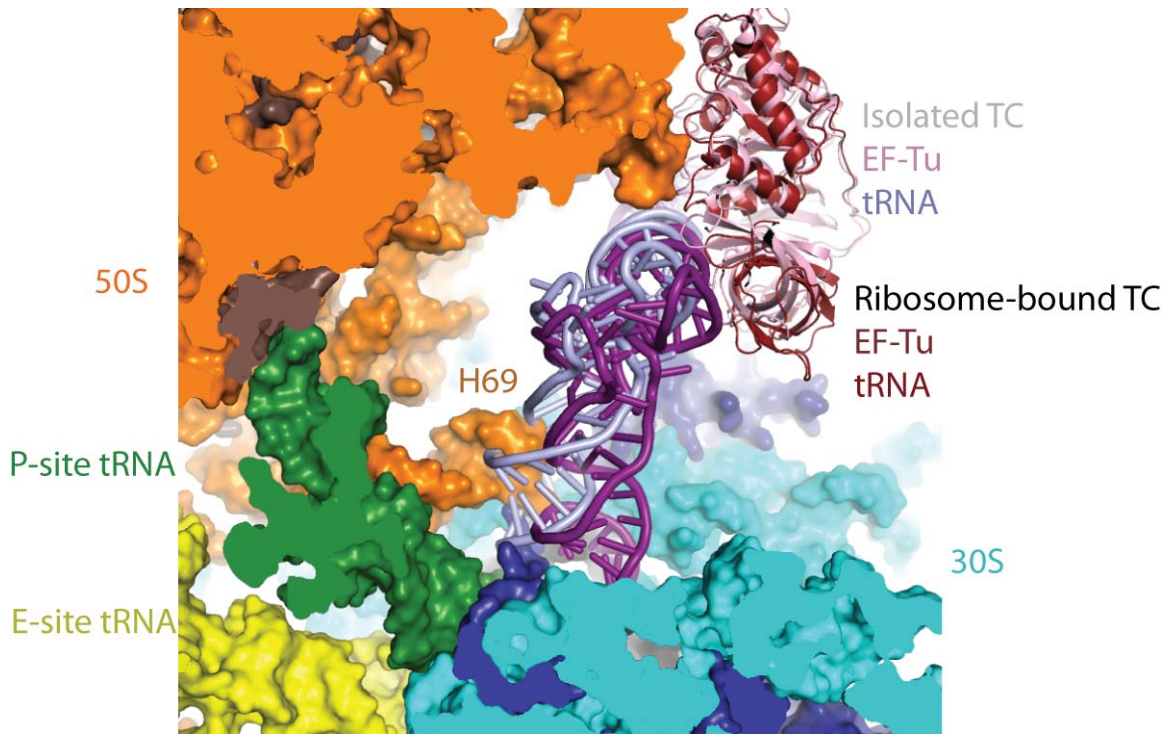


**fig. s3.** Superimposition of the isolated ternary complex and the ribosomal complex. When superimposed on domain 1 (GTPase domain), isolated TC (*II*) displays only minimal steric clashes with the ribosome. The most significant clash is with H69 of 23S rRNA, which is known to be mobile. Initial binding of TC is likely to involve a minimally distorted aminoacyl-tRNA conformation.

## References for Supplemental Information

1. Y. Gao *et al.*, *Science* 15 October 2009 (10.1126/science.1179709).
2. M. Selmer *et al.*, *Science* **313**, 1935 (2006).
3. J. C. Schuette *et al.*, *EMBO J.* **28**, 755 (2009).
4. S. Petry *et al.*, *Cell* **123**, 1255 (2005).
5. W. Kabsch, *J. Appl. Cryst.* **26**, 795 (1993).
6. A. T. Brünger *et al.*, *Acta Crystallogr. D Biol. Crystallogr.* **54**, 905 (1998).
7. R. M. Voorhees, A. Weixlbaumer, D. Loakes, A. C. Kelley, V. Ramakrishnan, *Nat. Struct. Mol. Biol.* **16**, 528 (2009).
8. P. V. Afonine, R. W. Grosse-Kunstleve, P. D. Adams, *CCP4 Newsl.* **42**, contribution 8 (2004).
9. H. Berchtold *et al.*, *Nature* **365**, 126 (1993).
10. T. Daviter, H. J. Wieden, M. V. Rodnina, *J. Mol. Biol.* **332**, 689 (2003).
11. P. Nissen *et al.*, *Science* **270**, 1464 (1995).

**Supplemental Movie 1.** Animation of decoding by the ribosome and EF-Tu. The incoming aminoacyl-tRNA, shown in purple, is delivered to the ribosome as part of a ternary complex with EF-Tu, shown in red, and GTP. This animation depicts the initial binding of the TC to the ribosome, followed by sampling of the mRNA codon and codon recognition. The animation then highlights the conformation changes in the 30S subunit, EF-Tu, and the 3' end of the aminoacyl-tRNA that provide the communication pathway between the decoding center of the 30S subunit and the GTPase center of EF-Tu. After hydrolysis of GTP and release of Pi, EF-Tu undergoes a domain rearrangement, leading to its dissociation and accommodation of the aminoacyl-tRNA into the peptidyl transferase center.